

IFJ-PAN-IV-2019-17  
August 30, 2022

# TAUOLA update for decay channels with $e^+e^-$ pairs in the final state.

S. Antropov<sup>a</sup>, Sw. Banerjee<sup>b</sup>, Z. Wąs<sup>a</sup>, J. Zaremba<sup>a</sup>

<sup>a</sup> *Institute of Nuclear Physics Polish Academy of Sciences , PL-31342 Krakow, Poland*

<sup>b</sup> *University of Louisville, Louisville, KY 40292, USA*

## ABSTRACT

With the arrival of high luminosity B-factories like the Belle II experiment,  $\tau$  decay measurements have become more precise than ever, allowing rarer processes to be explored, and finer details of  $\tau$  decays to be studied. These are important to understand the spectrum of intermediate particles produced in  $\tau$  decays. Therefore Monte Carlo generators, like the TAUOLA program, have to facilitate precision analysis as well as confront new models that constantly emerge with the availability of high statistics experimental data. New decay channels and models may lead to large variation of matrix elements size within the available phase space, as in the case when  $e^+e^-$  pairs are present in final state. It requires appropriate presampler of the phase space generator and a proper documentation to help users introduce their own models. While releasing a new update, it is important for the TAUOLA Monte Carlo library to maintain the general structure of the previous versions to preserve backward compatibility. The aim is to minimize changes from the user perspective. This paper presents a demonstration of new models implementation facilitated by the current update.

contact email: jakub.zaremba@ifj.edu.pl

# 1 Introduction

Thanks to its almost 30 years of long history, the **TAUOLA** [1, 2] Monte Carlo (MC) program maintains a large user community while facilitating present day experiments. Many solutions could not have been foreseen at the time of creation of the **TAUOLA** program. As users get accustomed to existing solutions the original structure of the program needs to be maintained, until an infrastructural update provides a major benefit. The high statistics data on  $\tau$  decays to be collected by the Belle II experiment brings new possibilities and challenges that nonetheless call for software adaptations.

One of the new aspects of  $\tau$  decay analysis is to search for rare Lepton Flavor Violating (LFV) decays. For this reason channels with photons and  $e^+e^-$  pairs are of interest, as they constitute the main source of Standard Model (SM) backgrounds to the LFV processes. This requires the presampler currently used in the phase space generation of **TAUOLA** program to be extended to accommodate for generation of new channels, in particular with  $e^+e^-$  pairs, where sharp peaks are present.

At the same time, old techniques [1] used to design experimental observable need to remain available. The MC generator must continue to be able to work in narrow width approximation for intermediate resonances, to ensure compatibility with analytical calculations.

It should be noted that in order to maintain the overall structure of the project, we have refrained from making drastic modifications e.g. ones that would change structure of specific arguments used by different functions and routines. This may seem to be sub-optimal from Information Technology point of view (especially if one ignores requirements of other programs), but can be justified from the point of view of physics complexity.

Our paper is organised as follows. In section 2 we explain how the phase space in **TAUOLA** is structured and parametrized. Section 3 introduces models which are useful for the technical tests of features expected in bremsstrahlung-like emission of  $e^+e^-$  pairs in the final state. Section 4 describes modifications of the phase space presampler required for this type of models with  $\tau$  decaying into 5 particles. Section 5 compares the performance of the new modifications of the phase space parameterization with the test matrix elements described in section 3. Different sets of initialization parameters for the presampler are discussed. These tests are important in the context of user modifications as they demonstrate how to optimize generation of the phase space density variation resulting from new models. It documents the “red flags” that we have

experienced, and describes the steps to be followed to resolve similar issues that can appear during phase space optimization by other users. Section 6 describes technical tests of the phase space presamplers. In section 7, we present examples of physical models implemented for:

- $\tau^- \rightarrow \pi^- e^- e^+ \nu_\tau$ ,
- $\tau^- \rightarrow \bar{\nu}_\mu \mu^- e^- e^+ \nu_\tau$ ,  $\tau^- \rightarrow \bar{\nu}_e e^- e^- e^+ \nu_\tau$ .

Selected plots and branching ratios (BR) calculated with the **TAUOLA** Monte Carlo are also presented. Section 8 summarizes the paper.

Some technical aspects of the paper are delegated to Appendices. Extended documentation of the presamplers may be required by the users. It is provided in the Appendix A. This is necessary since a lot of work on new models is expected from the growing user community. Introduction of decay channels with  $e^+ e^-$  pairs in the final state, requires not only extension of the presamplers but also new tests of technical and scientific nature. Technicalities are explained in Appendix B, but tests results are spread over Sections 3, 6 and 7.

## 2 Phase space generator structure

In the **TAUOLA** program, phase space generation and matrix element calculations are performed in separate units. Event construction starts from phase space. Through change of variables it can be optimized to generate more events in the regions where peaks of the matrix elements are expected. Finally, from the phase space Jacobian ( $J$ ) and the matrix element ( $\mathcal{M}$ ) a decay is simulated. The decay width is obtained using the canonical calculation:

$$d\Gamma = W * \prod_i^N dx_i, \quad (1)$$

where  $\{x_i\}$  denote set of random numbers and weight:

$$W = \frac{|\mathcal{M}|^2 * J}{2M_\tau}, \quad (2)$$

where  $M_\tau$  is the  $\tau$  lepton mass.

If weight is bigger than the random number multiplied by the maximum weight, event is accepted, otherwise it is rejected. We assume the reader is familiar with notation described in Ref [1].

Exact functional form of phase space Jacobians depends on the number of final state particles and parameterization chosen. Phase spaces are usually parametrized using Lorentz invariant quantities and angles of outgoing particles. In TAUOLA, the square of the invariant masses of systems of particles with descending number of decay products are used as the Lorentz invariant quantities<sup>1</sup>. For some matrix elements calculation, special features are expected in invariant masses like Breit-Wigner peaks. If no significant features are expected in the invariant mass squared  $s$ , the relevant coordinate of phase space is translated into a random number in [0,1] range using:

$$s = s_{min} + (s_{max} - s_{min}) \cdot x. \quad (3)$$

Let us call Eq. (3) a flat type coordinate presampler. If the matrix element contains a resonance in the variable  $s$ , we introduce a change of variable:

$$\begin{aligned} \alpha_{min} &= \arctan \frac{s_{min} - M_R^2}{\Gamma_R M_R}, \\ \alpha_{max} &= \arctan \frac{s_{max} - M_R^2}{\Gamma_R M_R}, \\ \alpha &= \alpha_{min} + (\alpha_{max} - \alpha_{min}) \cdot x, \\ s &= M_R^2 + \Gamma_R M_R \tan \alpha, \end{aligned} \quad (4)$$

where  $M_R$  and  $\Gamma_R$  are parameters describing the resonance present in the matrix element. Let us call Eq. (4) a resonant type phase space presampler<sup>2</sup>. If the resonance of the matrix element contributes with probability  $P$  to the total decay rate, then a numerically similar  $P$  can be used to mix phase space parameterizations as explained in Ref [1]. At the same time, values for  $M_R$  and  $\Gamma_R$  should be similar to mass and width of the resonance in matrix element. Therefore, phase space generation has parallel channels that correspond to the features of matrix element but use of their properties of should<sup>3</sup> not affect resulting distributions. Monte Carlo calculated partial

---

<sup>1</sup> For full functional forms we delegate reader to [1]. Here we would like to concentrate only on parts modifiable by the TAUOLA user through available tools for user re-definitions.

<sup>2</sup> We have checked that it is also convenient to compensate for matrix element peak of e.g.  $\gamma^* \rightarrow e^+ e^-$  propagator, then  $M_R = 2m_e$  and  $\Gamma_R = 2m_e$  is used.

<sup>3</sup> Use of resonant type phase space presampler compensates for peaks in matrix element.

width and its uncertainty are accurately calculated as long as significant amount of over-weighted events are not generated. If the correspondence is poor, and somewhat different values of  $P$ ,  $M_R$  and  $\Gamma_R$  are present in the matrix element calculation than in phase space parameterization, event generation will suffer from low efficiency<sup>4</sup>. Large number of over-weighted events relative to the sample size and big uncertainty on partial width are signs that features of matrix element and phase space generation do not adequately correspond to each other.

Whenever a change of variable is performed, the Jacobian of a such change enters into the phase space formula. In our case we have multiple channels in presampler, which with necessitates multiple change of variables. This can be taken into account by introducing harmonically averaged Jacobian ( $J_{total}$ ) from  $n$  different channels in the presampler:

$$\frac{1}{J_{total}} = \sum_{i=1}^n \frac{P_i}{J_i}, \quad (5)$$

where  $P_i$  is the probability of the  $i^{th}$  presampler channel, and  $J_i$  is the Jacobian corresponding to change of variable performed for the  $i^{th}$  channel.

We delegate Appendix A to detailed information on the presampler channels and the parameterization types used. We would like to stress that presampler parameters need to be tailored for each decay channel separately.

### 3 Features expected in matrix element

Before introducing any changes to phase space generator we would like to discuss what to expect from channels with bremsstrahlung of pair emission. For this purpose, we have chosen models for  $\tau^- \rightarrow \pi^- e^- e^+ \nu_\tau$  as in Ref. [3] and for  $\tau^- \rightarrow \bar{\nu}_\mu \mu^- e^- e^+ \nu_\tau$  we considered an approach of factorizing the matrix element for pair emission. Both predict dominant contribution from near real photon, manifesting as extremely large peak in  $e^- e^+$  mass spectra. This can be simplified<sup>5</sup> to the matrix element:

$$\mathcal{M} = \frac{1}{k^2}, \quad (6)$$

---

<sup>4</sup> Number of accepted events divided by number of generated events.

<sup>5</sup> We opt for simplified model only for testing purposes, as it is then clear what we are testing. Otherwise, introducing physical models right away might hinder tests in an unpredictable manner.

where  $k = P_{e-} + P_{e+}$ . Acollinearity<sup>6</sup> of emitted pair with the third charged particle in the  $\tau$  decay is the next feature to be addressed. We model this feature with a minor extension to the previous equation:

$$\mathcal{M} = \frac{1}{k^2} \frac{2P_1}{(2P_1 \cdot k + k^2)}, \quad (7)$$

where  $P_1$  is four momentum of the third charged particle (either  $\pi^-$  or  $\mu^-$ ). By comparing the above equation to e.g. Eq. 2 of Ref. [3], one can see that this is a simplified form of bremsstrahlung only from the final state. Eq. (6) and Eq. (7), while being far away from fully describing the complete underlying processes, are convenient for testing, and will be used in following sections to illustrate the relevant subtle points. They can be easily integrated analytically and numerically. In Appendix B we use similarly simplified models (e.g.  $\mathcal{M} = \frac{\text{const.}}{k}$ ) for testing the numerical stability of factorization of the bremsstrahlung part of full matrix element. It further validates use of matrix elements presented in this section.

## 4 Enhancing phase space presampler for 5-particle decays

From the considerations of the previous section, we can conclude that it is important for the presampler to accommodate for the peaks in the mass of two particles<sup>7</sup>. The phase space presampler for 5-particle decays used to have only two channels, where resonant type parameterization as described by Eq. (4) was used only for the invariant mass of three particles: ( $2^{\text{nd}}$ ,  $3^{\text{rd}}$  and  $4^{\text{th}}$ ) or ( $1^{\text{st}}$ ,  $3^{\text{rd}}$  and  $4^{\text{th}}$ ). This is insufficient for a decay such as  $\tau^- \rightarrow \bar{\nu}_\mu \mu^- e^- e^+ \nu_\tau$ , which clearly requires resonant type presampler in the invariant mass of two particles.

To introduce new phase space channel we internally defined<sup>8</sup> enhancement for both mass and width of resonance, set to<sup>9</sup> 0.001 GeV ( $\sim 2m_e$ ). New channel

---

<sup>6</sup> Confirming that this acollinearity is handled well means that acollinearity of photon in channels with  $\gamma$  in the final state also can be modeled adequately.

<sup>7</sup> Ordering of particles is important here. Last particle is always assumed to be  $\nu_\tau$ . We choose here to put  $e^-$  and  $e^+$  as the  $3^{\text{rd}}$  and  $4^{\text{th}}$  daughter.

<sup>8</sup> We want to minimize changes to the phase space generator as well as user interface. Introducing new arguments for the routine is therefore at present undesirable.

<sup>9</sup> It is good enough for the low mass enhancement and in future can be immediately used for narrow resonances in other channels.

is activated with probability of 0.8 if the 3<sup>rd</sup> and the 4<sup>th</sup> particle in the decay are  $e^-$  and  $e^+$ , respectively. Such choice greatly improved efficiency of generation of demo model as detailed in section 5.1. Appendix A.2 documents the new structure of this presampler.

## 5 Presampler parameters optimization

While adding new decay channels through the interface for user re-definitions of TAUOLA, it is important to keep in mind that presampler parameters can account for the newly introduced matrix elements. For our demo model of Eq. (6) that means optimizing the parameters for peak in the low mass region of invariant mass of  $e^+e^-$  pair. In this section we will show how the choice of parameters may influence event generation. We should note that such choice doesn't need to be perfect as it affects only the efficiency of event generation. Usually it is not worth putting in more effort into searching of optimal parameter values if the efficiency exceeds 10% and not too many<sup>10</sup> over-weighted events are generated. That being said, for complicated channels with high multiplicity in final state particles, high efficiencies might be unattainable.

### 5.1 Case of $\tau^- \rightarrow \bar{\nu}_\mu \mu^- e^- e^+ \nu_\tau$

Prior to introduction of the enhancement described in Section 4, the structure of phase space presampler for decays into 5 particles was insufficient and suffered from up to 48% of over-weighted events. This happened due to lack of phase space for the resonant type parameterization in the invariant mass constructed from four-momenta of two particles. Historically this presampler was used for channels with 4 hadrons only in the final state. In such cases, formation of narrow resonance in the mass of two particles was not expected<sup>11</sup>. No known hadronic current featured such resonances at the time. The need

---

<sup>10</sup> Relative to the sample size and specific matrix elements. Usually if less than 1% of the events are over-weighted, it is acceptable. If it is more, then we suggest double checking the matrix element and the chosen presampler parameters. One should also check if there are any deformations in generated distributions.

<sup>11</sup> Mass of 4 hadrons is relatively high, therefore there is little phase space available for creation of such resonance, especially assuming all 4 hadrons come from  $a_1$  decay into  $\rho\pi$  and subsequent decay of  $\rho \rightarrow \pi\pi\pi$ .

has arisen only now with advent of high precision data from experiments like Belle II, allowing for investigation of rare decays.

In this subsection we present results from optimization of parameters for the channel newly added to the presampler. Table 1 collects information on how the probability of resonance-like phase space enhancement branch in mass of  $e^+e^-$  affects the efficiency of event generation. At the same time it barely affects the calculated partial width (see Table 1), which is how it should be. Tests were performed on a sample of 10M events. Figure 1 compliments these results with example plots obtained by comparing the optimized presampler (probability = 0.8) to the old one (probability = 0.0). Plots were obtained with the help of MC-TESTER [4, 5]. The differences are large, exposing the impact from over-weighted faulty events obtained while using the old presampler.

Presampler param.	Presampler performance			
Probability	Efficiency	over-weighted	width [GeV]	relative error
0.0	0.0005	48%	$0.13784 \cdot 10^{-2}$	0.00204682
0.2	0.036	0	$0.13747 \cdot 10^{-2}$	0.00014140
0.4	0.066	0	$0.13742 \cdot 10^{-2}$	0.00012545
0.6	0.099	0	$0.13744 \cdot 10^{-2}$	0.00011399
0.8	0.132	0	$0.13741 \cdot 10^{-2}$	0.00010129

Table 1: Probability of internally defined phase space channel and resulting efficiency of generation for demonstrative  $\tau^- \rightarrow \bar{\nu}_\mu \mu^- e^- e^+ \nu_\tau$  decay as defined by Eq. (6). Tests were done with sample size of 10M events.

## 5.2 Case of $\tau^- \rightarrow \pi^- e^- e^+ \nu_\tau$

In this subsection we want to present procedure for optimizing parameters of presampler for decays into 4 particles. From the matrix element for our demo model (Eq. (6)) and presampler structure (Appendix A.3), we may conclude that we need modify presampler parameters to facilitate the  $e^-e^+$  peak with relatively high probability. Other parameters are of secondary importance and should correspond to roughly flat phase space. Table 2 collects selected values of presampler parameters and their resulting efficiency. Parameters  $P_A$ , MA, GA were left at default values<sup>12</sup>, and therefore are not listed in the table.

<sup>12</sup> That is  $P_A = 0.0$ , therefore MA and GA are irrelevant

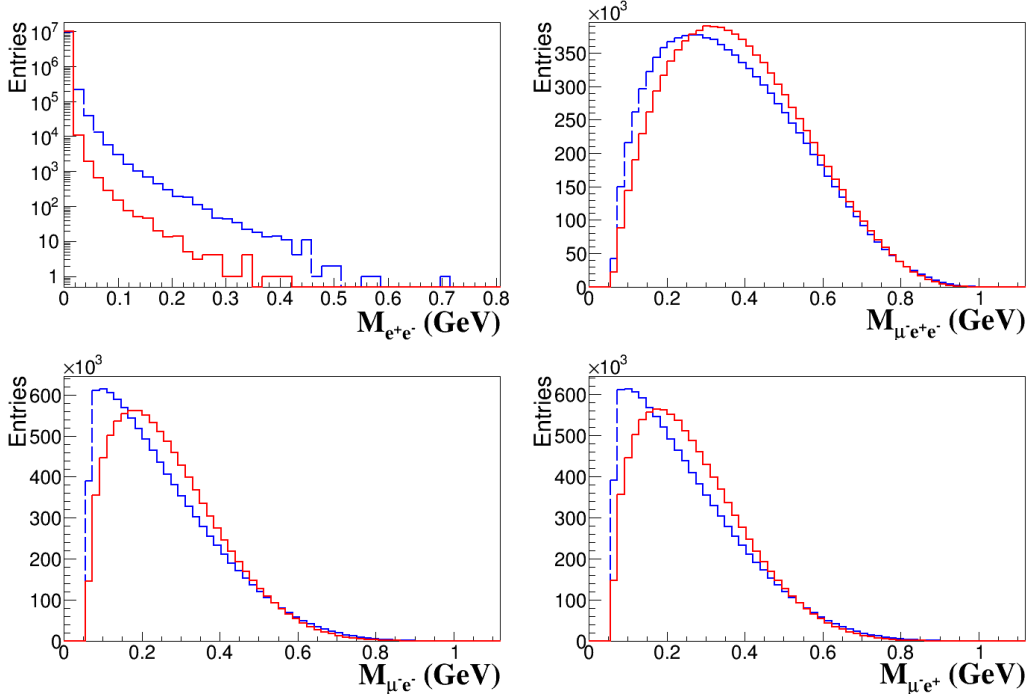


Figure 1: Example plots from MC-TESTER [4, 5]: comparison for  $\tau^- \rightarrow \bar{\nu}_\mu \mu^- e^- e^+ \nu_\tau$  decay modeled with Eq. (6) with different phase space parameters, as listed in Table 1. Invariant masses of  $e^+e^-$ ,  $\mu^-e^+e^-$ ,  $\mu^-e^-$  and  $\mu^-e^+$  systems are shown on top-right, top-left, bottom-left and bottom-right, respectively. These plots show an extreme case where the presampler parameters are completely disconnected from matrix element used, and therefore shapes of the plots are affected. Dashed blue line represents plots with probability = 0.0, which is same as using unmodified phase space generator, while solid red line is obtained while using probability = 0.8. Large differences in the distributions come from high amount (48%) of over-weighted events in sample generated with probability = 0.0. Samples of 10M events were used for this comparison.

Without any optimization of presampler the  $\tau^- \rightarrow \pi^- e^- e^+ \nu_\tau$  channel had an efficiency of generation at the level of 0.00024, with over 45% over-weighted events. Such results are unacceptable, and values of partial width and its error collected in Table 2 have little meaning on the shapes of the distributions when so many over-weighted events are present. Fortunately, in this case, all relevant presampler channels are available and it is enough to modify parameters through interface of **TAUOLA-bbb** via user re-definitions.

Table 2 collects information on how the probability of branch with resonance-like enhancement of phase phase in the mass of  $e^+ e^-$  affects efficiency of generation. Figure 2 compares with the help of MC-TESTER [4, 5] selected mass distributions<sup>13</sup> obtained with old (first line in Table 2) and optimized (last line in Table 2) parameters of the presampler. Figure 3 presents similar comparison between samples obtained with presampler parameters set to the second last and the last set of values listed in Table 2.

Presampler param.					Presampler performance			
$P_B$	MX	GX	MB	GB	eff.	overw.	width[GeV]	rel.error
0.0	1.251	0.599	0.7759	0.1479	0.00024	45%	0.616/NaN	0.2423/NaN
0.5	1.251	0.599	0.001	0.001	0.0458	0% (14)	0.424	0.0006
0.5	1.251	0.7	0.001	0.001	0.0519	0% (8)	0.427/NaN	0.0035/NaN
0.5	1.0	0.7	0.001	0.001	0.0912	0% (10)	0.425	0.0001
0.5	0.9	0.8	0.001	0.001	0.1258	0% (11)	0.426	0.0010
0.8	0.9	0.8	0.001	0.001	0.1943	0% (1)	0.425	0.0001

Table 2: Presampler parameters and resulting efficiency of generation, over-weighted events, width and relative error of the width for demo model of  $\tau^- \rightarrow \pi^- e^- e^+ \nu_\tau$  decay. First line corresponds to initialization as of previous **TAUOLA** versions. Set of parameters with the best efficiency is considered the optimal one. Sample size of 10M events was used. Unphysical models can sometimes result in NaN value from matrix element calculation. Even one such unphysical event in generation renders width and its error to be NaN. In case when NaN are obtained in samples of 10M events, values obtained with a smaller set of 10k sample, which avoids generation of the unphysical event, are listed. As these are only demonstrative models and such events happen due to sub-optimal parameterization, it is not worth resolving the issue.

---

<sup>13</sup> MC-TESTER compares all possible invariant mass distributions. We do not think presenting all of them here is beneficent to the reader, therefore we select only few plots.

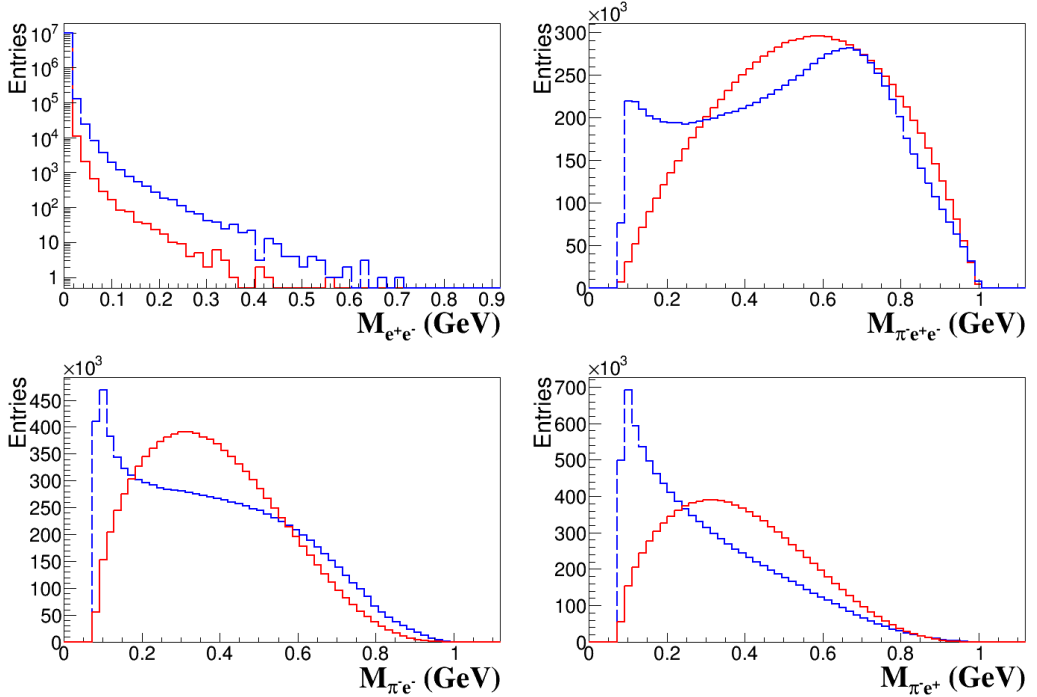


Figure 2: Example plots from MC-TESTER [4, 5]: comparison for  $\tau^- \rightarrow \pi^- e^- e^+ \nu_\tau$  decay modeled with Eq. (6). Invariant masses of  $e^+e^-$ ,  $\pi^-e^+e^-$ ,  $\pi^-e^-$  and  $\pi^-e^+$  systems are shown on top-right, top-left, bottom-left and bottom-right, respectively. Dashed blue line represents plots before any changes to phase space parameters and solid red lines show best set of parameters, as listed in Table 2. Large differences in the distributions come from high number of over-weighted events (45%) in sample generated with unmodified phase space parameters. Samples of 10M events were used for this comparison.

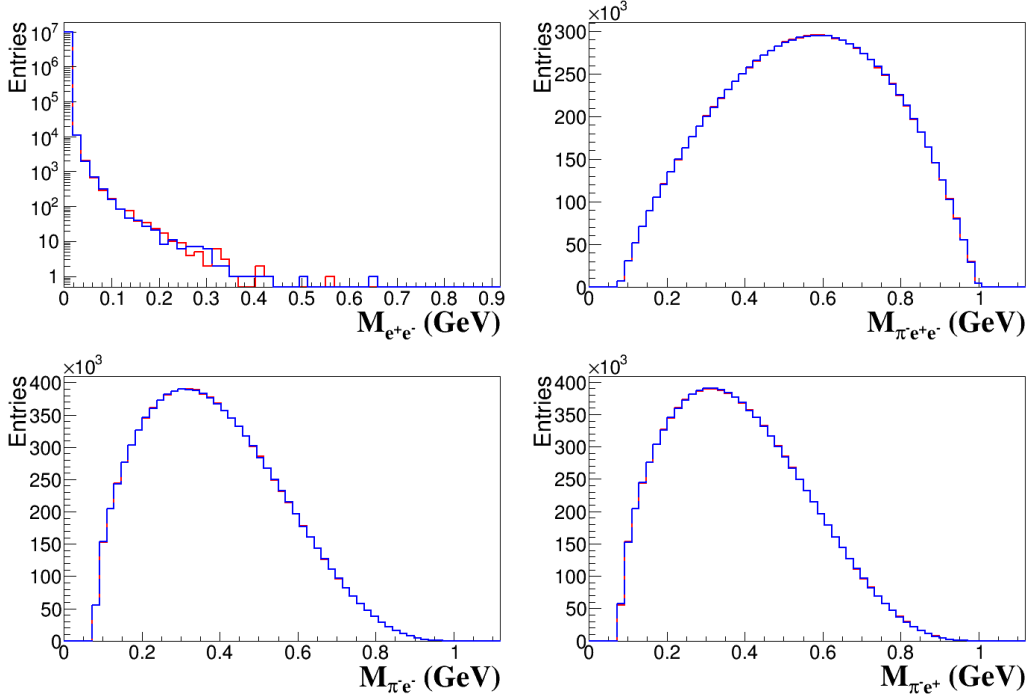


Figure 3: Example plots from MC-TESTER [4, 5]: comparison for  $\tau^- \rightarrow \pi^- e^- e^+ \nu_\tau$  decay modeled with Eq. (6) with different phase space parameters chosen (see Table 2 for all tested sets of parameters). Invariant masses of  $e^+e^-$ ,  $\pi^-e^+e^-$ ,  $\pi^-e^-$  and  $\pi^-e^+$  systems are shown on top-right, top-left, bottom-left and bottom-right, respectively. Dashed blue line represents plots with sub-optimal phase space parameters choice ( $P_B = 0.5$ ,  $MX=1.251$ ,  $GX=0.599$ ,  $MB=0.001$ ,  $GB=0.001$ ), while the solid red line is obtained with best found set of parameters ( $P_B = 0.8$ ,  $MX=0.9$ ,  $GX=0.8$ ,  $MB=0.001$ ,  $GB=0.001$ ). Lack of significant differences for these and all other plots is a proof that presampler works correctly, that is parameters (as long as they are within reasonable range) affect only efficiency of generation and do not affect shapes of the distributions. Samples of 10M events were used for this comparison.

The main aspect of optimizing presampler is reducing number of over-weighted events, as these hinder calculation of partial width along with its error, and in extreme cases alter shapes of distributions. With sample of 10k events we obtain partial width of 0.616 GeV and relative error of 0.242 for the old presampler, while after optimization of the parameters we get width of 0.425 GeV and error of 0.003 with same sample size. Note that investigated demonstrative model is unphysical and so is obtained partial width. The takeaway message from this exercise is the impact of presampler parameters on error estimation. With the results collected so far, we can conclude that narrow width resonance structure which we used in phase space enhancement is sufficient to handle the logarithmic structure of  $e^-e^+$  pseudo-singularity. This is not unexpected because the propagator of resonance:  $1/(s + M^2)$  in the limit of  $s \gg M^2$  resembles the propagator  $1/s$  in our demo model.

### 5.3 Investigating acollinearity of emitted pair

The demo model of Eq. (6) emulates the most important feature of the models containing  $e^+e^-$  pair of the final state, which manifests as a soft singularity. Eq. (7) emulates in addition a secondary feature, e.g. collinear singularity of the emitted pair. In terms of the invariant masses, this should result in narrow peak in the mass of three charged particles of the final state. Fig. 4 and Fig. 5, compare the distributions obtained with models of Eq. (6) and Eq. (7) for  $\tau^- \rightarrow \pi^-e^-e^+\nu_\tau$  and  $\tau^- \rightarrow \bar{\nu}_\mu\mu^-e^-e^+\nu_\tau$  decays, respectively, and show that this is indeed the case.

As expected, generating events with new matrix element of Eq. (7) brought back the problem of low efficiency of generation. We concentrate on parameters for invariant mass of three charged particles<sup>14</sup>, as this is where the new peak appears.

In Tab. 3 we collect the results for  $\tau^- \rightarrow \pi^-e^-e^+\nu_\tau$  decay. We can see there that some over-weighted events remain even for well optimized phase space parameters, and we get over 30% efficiency of generation, which is very much acceptable.

In Tab. 4 we collect the results for  $\tau^- \rightarrow \bar{\nu}_\mu\mu^-e^-e^+\nu_\tau$  decay. We can

---

<sup>14</sup> Note that phase space generator for 5 particles has only resonant type phase space parameterization in the mass of four particles ( $\nu_\tau$  excluded). By default parameters there are set to MR=1.251 and GR=0.599. Leaving those parameters unmodified is appropriate for flat phase space. There is no need to add new presampler channel for the mass of 4 particles.

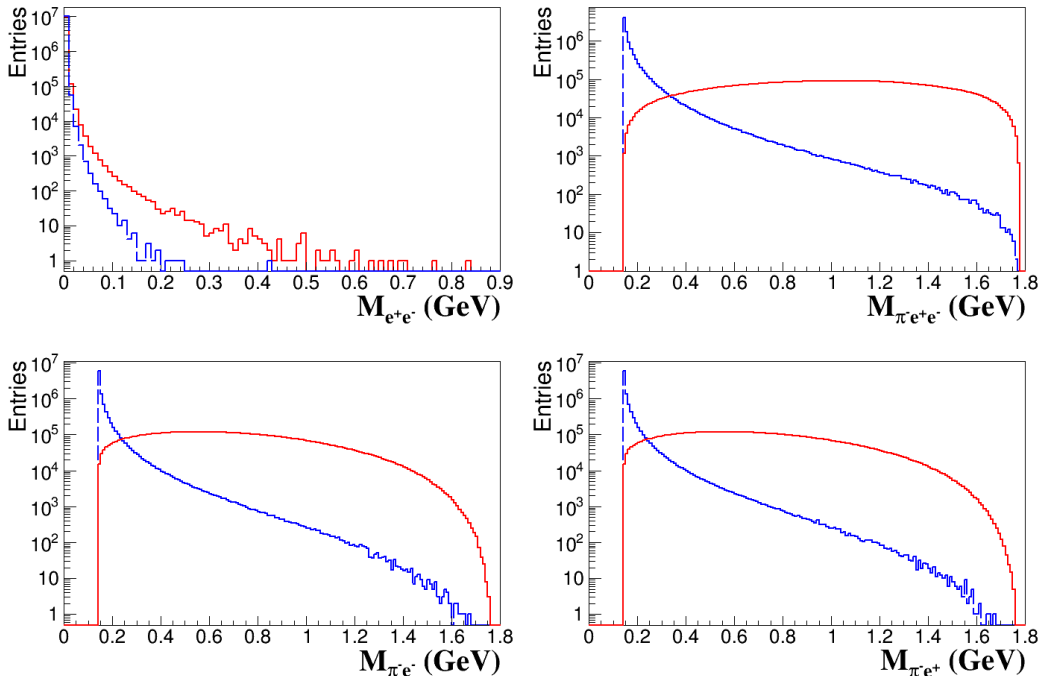


Figure 4: Example plots from MC-TESTER [4, 5]: comparison for  $\tau^- \rightarrow \pi^- e^- e^+ \nu_\tau$  decay. Dashed blue line represents model of Eq. (7) and solid red line models Eq. (6). Invariant masses of  $e^+ e^-$ ,  $\pi^- e^+ e^-$ ,  $\pi^- e^-$  and  $\pi^- e^+$  systems are shown on top-right, top-left, bottom-left and bottom-right, respectively. We can see that extended matrix element resulted in (as expected) peaks in invariant mass of  $\pi^- e^- e^+$  and  $\pi^- e^+$ ,  $\pi^- e^-$  systems. Samples of 10M events were used for this comparison.

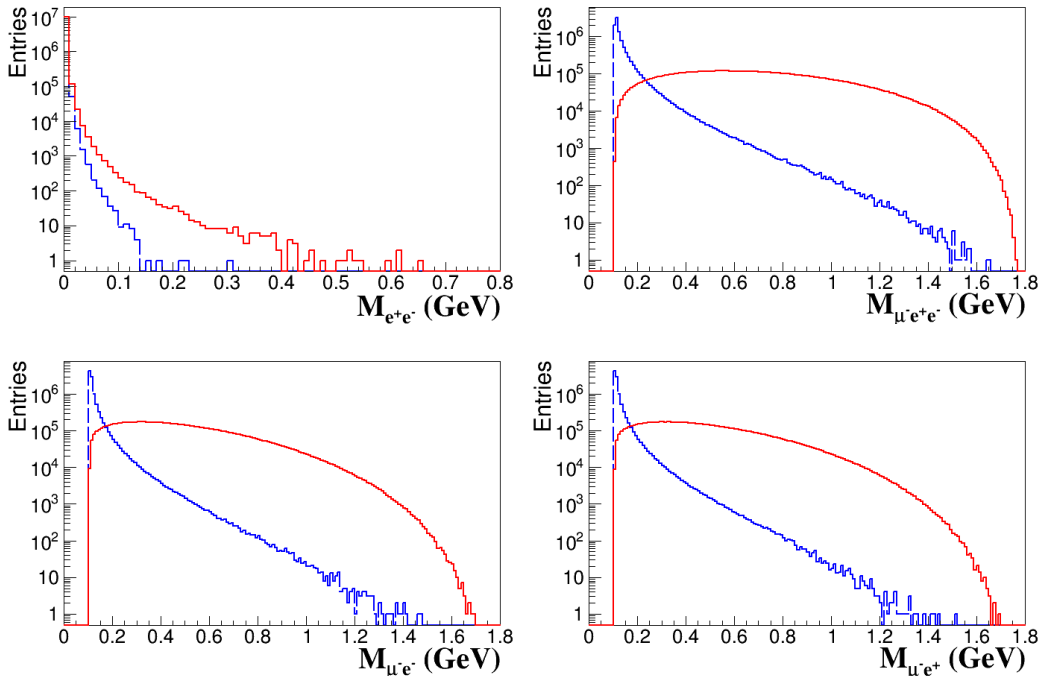


Figure 5: Example plots from MC-TESTER [4, 5]: comparison for  $\tau^- \rightarrow \bar{\nu}_\mu \mu^- e^- e^+ \nu_\tau$  decay. Dashed blue (light grey) line represents model of Eq. (7) and solid red (dark grey) line models Eq. (6). Invariant masses of  $e^+e^-$ ,  $\mu^-e^+e^-$ ,  $\mu^-e^-$  and  $\mu^-e^+$  systems are shown on top-right, top-left, bottom-left and bottom-right, respectively. We can see that extended matrix element resulted in (as expected) peaks in invariant mass of  $\mu^-e^-e^+$  and  $\mu^-e^+$ ,  $\mu^-e^-$  systems. Samples of 10M events were used for this comparison.

Presampler param.		Presampler performance			
MX	GX	eff.	overw.	width[GeV]	rel.error
0.9	0.8	0.001	0% (12)	3.2315/NaN	0.0052/NaN
0.2	0.2	0.029	0% (6)	3.7326	0.0001
0.17	0.1	0.068	0% (5)	3.7316	0.0001
0.15	0.05	0.190	0% (6)	3.7315	0.0001
0.13	0.05	0.305	0% (9)	3.7317	0.0001

Table 3: Presampler parameters, resulting efficiency of generation, over-weighted events, width and relative error of the width for demo model of  $\tau^- \rightarrow \pi^- e^- e^+ \nu_\tau$  decay. Sample size of 10M events was used. In case of NaN obtained with 10M sample, values obtained with 10k sample are given.

see there that efficiency of generation is somewhat poor ( 6%). This should not trouble us too much as channels with higher multiplicity of final state particles tend to have lower efficiency of generation. For more complicated models, the efficiency should drop even more.

Presampler param.			Presampler performance			
$P_A$	MA	GA	eff.	overw.	width[GeV]	rel.error
0.0	0.7759	0.1479	0.003	8% (886001)	$0.3230 \cdot 10^{-1}$	0.0001
0.6	0.17	0.1	0.003	0% (0)	$0.3230 \cdot 10^{-1}$	0.0001
0.7	0.15	0.05	0.015	0% (0)	$0.3231 \cdot 10^{-1}$	0.0001
0.8	0.105	0.005	0.060	0% (0)	$0.3231 \cdot 10^{-1}$	0.0001

Table 4: Presampler parameters, resulting efficiency of generation, over-weighted events, width and relative error of the width for demo model of  $\tau^- \rightarrow \bar{\nu}_\mu \mu^- e^- e^+ \nu_\tau$  decay. Sample size of 10M events was used. For results documented here we used MR=1.0 and GR=0.9.

## 6 Phase space presamplers tests

With the introduction of the new channels featuring  $e^+e^-$  pair (as well as channels with photon) in the final state, the question of numerical precision

arose. Similar to the case of PHOTOS Monte Carlo [6], double precision accuracy is now necessary for generation of phase space in TAUOLA.

There are 6 phase space generators used for each group of decay channels with a specific amount of final state particles. These are generators for 2, 3, 4, 5, 6 and N particles, where the last one supports up to 9 particles. Special generator introduced for  $\tau \rightarrow \ell \nu_\ell \bar{\nu}_\tau (\gamma)$  decays does not need to be modified by the user. As the arguments of routines and parameters in the library uses float precision, we chose a solution that maintains backward compatibility. Arguments for phase space generation routines remain float, while all the calculations within, are performed in double precision. Such procedure guarantees that any models developed for the previous TAUOLA release work right away, without any modifications.

For validation of the changes we have used MC-TESTER to confirm that no technical problem arises in any of decay channels present in TAUOLA due to updates from this paper. The Shape Difference Parameter (SDP), for exact definition see Section 4 of [4], for all distributions are equal to 0. This was tested for each channel separately, for groups of channels, as well as for a run where all the channels are generated simultaneously, with sample sizes at least of 10M events for each run. As an example, Fig. 6 from tests of  $\tau$  decay to 5 particles are presented, using a generated sample of 100M events, which gives almost 4M events for each decay channel of similar type. The whole test consists of hundreds of histograms, while the upgrade to double precision itself is quite straightforward.

## 7 Implementation example

Ref. [3] (Eq. 31) provides formula for bremsstrahlung of pair emission which has been introduced for physical modeling for pair emission into TAUOLA. Implementation can thus be cross-checked with analytical results.

For the case of  $\tau^- \rightarrow \pi^- e^+ e^- \nu_\tau$  decays, Ref. [3] predicts branching ratio of  $(1.461 \pm 0.0006) \times 10^{-5}$ , the Belle collaboration reports [7] branching ratio between  $(1.46 \pm 0.13 \pm 0.21) \times 10^{-5}$  and  $(3.01 \pm 0.27 \pm 0.43) \times 10^{-5}$ , while our MC simulation produces a result of  $(1.398 \pm 0.001) \times 10^{-5}$ . In case of  $\tau^- \rightarrow \pi^- \mu^+ \mu^- \nu_\tau$ , Ref. [3] gives branching ratio of  $(1.6 \pm 0.007) \times 10^{-7}$ , while the Belle collaborations quotes an upper limit of  $1.14 \times 10^{-5}$  at 90% confidence level. Our MC simulation produces  $(1.035 \pm 0.003) \times 10^{-7}$ . Those results seem to be in reasonable agreement and are collected in Table 5.

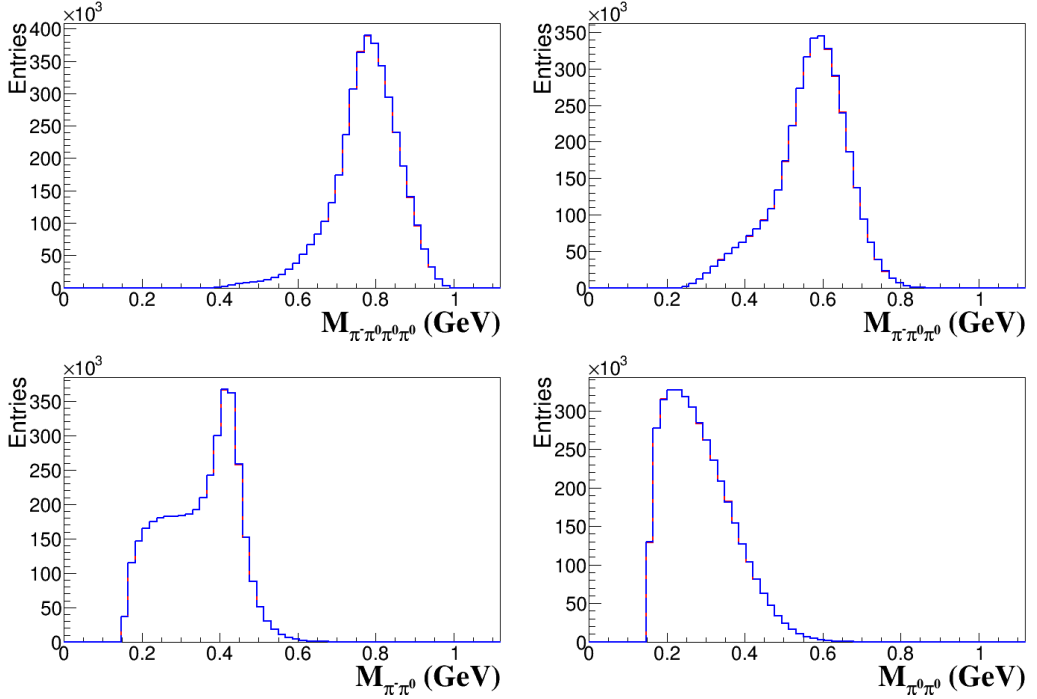


Figure 6: Example plots from MC-TESTER [4, 5]: comparison of channels that could be affected by changes introduced into phase space generator for decays into 5 particles. Dashed blue lines represent the plots before changes and the solid red lines model the shapes after introduction of double precision. Shown are selected plots for  $\tau^- \rightarrow \pi^-\pi^0\pi^0\pi^0\nu_\tau$  decay channel with the original and updated code. Invariant masses of  $\pi^-\pi^0\pi^0\pi^0$ ,  $\pi^-\pi^0\pi^0$ ,  $\pi^-\pi^0$  and  $\pi^0\pi^0$  systems are shown on top-right, top-left, bottom-left and bottom-right, respectively. Full comparison contains dozens of similar plots and features SDP=0 (see Section 4 of [4]) for all of them.

Decay mode	theoretical BR	Monte Carlo BR	experimental BR
$\tau^- \rightarrow \pi^- e^+ e^- \nu_\tau$	$(1.461 \pm 0.0006) \times 10^{-5}$	$(1.396 \pm 0.0004) \times 10^{-5}$	$< 3.01^{+0.27+0.43}_{-0.27-0.43} 10^{-5}$
$\tau^- \rightarrow \pi^- \mu^+ \mu^- \nu_\tau$	$(1.6 \pm 0.0003) \times 10^{-7}$	$(1.038 \pm 0.0003) \times 10^{-7}$	$< 1.14 \times 10^{-5}$

Table 5: Comparison of branching ratios obtained from our MC implementation of model based on Ref [3] with theoretical prediction (from the above-mentioned reference) and experimental results from the Belle experiment [7].

There are multiple possible sources of the remaining differences: phase space approximation in analytical calculations consistent with matrix element; exact phase space used in MC generation; differences in parameters values; values of masses of intermediate particles,  $|V_{ud}|$ , etc. Selected distributions of invariant mass obtained from our simulation are shown in Fig 7.

In the case of  $\tau^- \rightarrow \bar{\nu}_\mu \mu^- e^- e^+ \nu_\tau$  and  $\tau^- \rightarrow \bar{\nu}_e e^- e^- e^+ \nu_\tau$  decays we use matrix element squared described by the following factorized form:

$$|\mathcal{M}|^2 = |\mathcal{M}(\tau \rightarrow \ell \nu_\ell \nu_\tau)|^2 \cdot 2e^4 \frac{4p_e^\alpha p_{e+}^\beta - k^2 g^{\alpha\beta}}{k^4} \left( \frac{p_\ell}{kp_\ell} - \frac{p_\tau}{kp_\tau} \right)_\alpha \left( \frac{p_\ell}{kp_\ell} - \frac{p_\tau}{kp_\tau} \right)_\beta, \quad (8)$$

where  $\ell$  denotes a light lepton (electron or muon) and  $\alpha, \beta$  are Lorentz indices. With this we have run multiple technical tests, details of which are described in Appendix B. We conclude that with such a physical model<sup>15</sup>, the results are in reasonable agreement with those obtained by the CLEO experiment [8]. We collect the results in Table 6 along with the values from theoretical calculations published in Ref. [9]. Selected distributions of invariant mass obtained from our simulation are shown in Fig 8.

Decay mode	theoretical BR	Monte Carlo BR	experimental BR
$\tau^- \rightarrow \bar{\nu}_\mu \mu^- e^- e^+ \nu_\tau$	$(4.21 \pm 0.01) \times 10^{-5}$	$(1.538 \pm 0.0005) \times 10^{-5}$	$< 3.2 \times 10^{-5}$ (at 90% C.L.)
$\tau^- \rightarrow \bar{\nu}_e e^- e^- e^+ \nu_\tau$	$(1.984 \pm 0.004) \times 10^{-5}$	$(2.871 \pm 0.0004) \times 10^{-5}$	$2.7^{+1.5+0.4+0.1}_{-1.1-0.4-0.3} 10^{-5}$

Table 6: Comparison of branching ratios obtained from MC implementation of our model (8) with theoretical prediction from Ref. [9] and experimental results from the CLEO experiment [8].

<sup>15</sup> We assume soft pairs, therefore we can start from the matrix element for leptonic  $\tau$  decays and multiply it by a factor for pair emission.

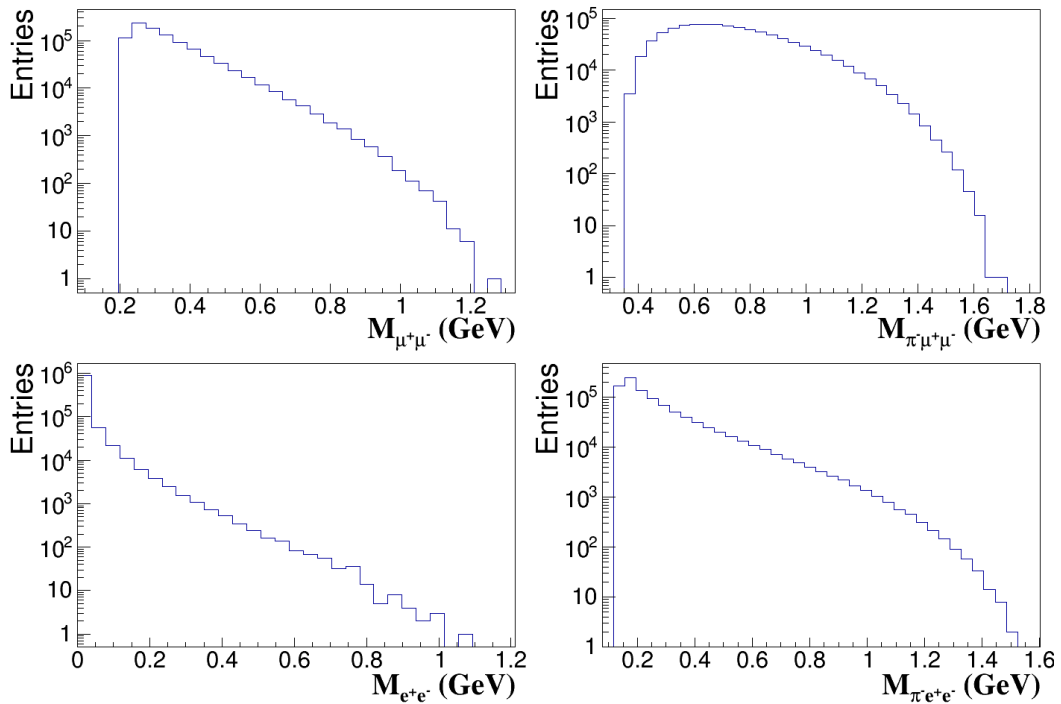


Figure 7: Invariant masses of  $\mu^+\mu^-$  and  $\pi^-\mu^+\mu^-$  systems in  $\tau^- \rightarrow \pi^-\mu^+\mu^-\nu_\tau$  decays are shown on top-left and top-right, and those of  $e^+e^-$  and  $\pi^-e^+e^-$  systems in  $\tau^- \rightarrow \pi^-e^+e^-\nu_\tau$  decays on bottom-left and bottom-right, respectively. Plots obtained from MC samples of 4M events.

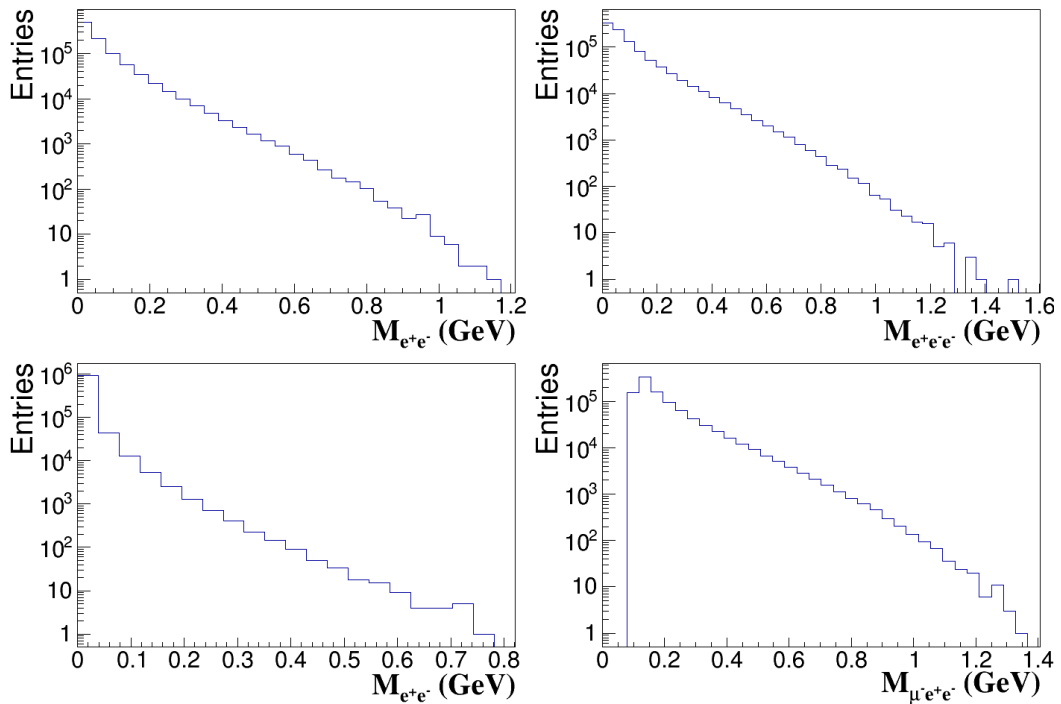


Figure 8: Invariant masses of  $e^+e^-$  and  $e^-e^+e^-$  systems in  $\tau^- \rightarrow \bar{\nu}_e e^- e^+ e^- \nu_\tau$  decays are shown on top-left and top-right, and those of  $e^+e^-$  and  $\mu^-e^+e^-$  systems in  $\tau^- \rightarrow \bar{\nu}_\mu \mu^- e^+ e^- \nu_\tau$  decays on bottom-left and bottom-right, respectively. Plots obtained from MC samples of 4M events.

## 8 Summary

In this paper we document the motivation for a new TAUOLA release, and its modifications. The main purpose of this new version is to facilitate models for generation of previously unconsidered features in phase space arising from logarithmic peaks of infrared and acollinear nature in bremsstrahlung-like emission, as opposed to standard Breit-Wigner ones. This is necessary to properly introduce models to study the background from  $\tau$  decays in searches of New Physics. Also in this paper we provide a more complete documentation for TAUOLA-**bbb** [2] in terms of the phase space presamplers. This is for convenience to the user community to exploit all features of this tool. Finally, we document new tests of TAUOLA and its interface for user-defined models. Examples of matrix elements based on ref. [3] along with analytical and numerical calculations are confronted and presented. More technical aspects and supplementary tests are delegated to Appendices.

### Acknowledgments

This project was supported in part from funds of Polish National Science Centre under decisions DEC-2017/27/B/ST2/01391.

## References

- [1] S. Jadach, Z. Was, R. Decker, and Johann H. Kuhn. The tau decay library TAUOLA: Version 2.4. *Comput. Phys. Commun.*, 76:361–380, 1993.
- [2] M. Chrzaszcz, T. Przedzinski, Z. Was, and J. Zaremba. TAUOLA of  $\tau$  lepton decays—framework for hadronic currents, matrix elements and anomalous decays. *Comput. Phys. Commun.*, 232:220–236, 2018.
- [3] A. Guevara, G. Lopez Castro, and P. Roig. Weak radiative pion vertex in  $\tau^- \rightarrow \pi^- \nu_\tau \ell^+ \ell^-$  decays. *Phys. Rev.*, D88(3):033007, 2013.
- [4] P. Golonka, T. Pierzchala, and Z. Was. MC-TESTER: A Universal tool for comparisons of Monte Carlo predictions for particle decays in high-energy physics. *Comput. Phys. Commun.*, 157:39–62, 2004.
- [5] N. Davidson, P. Golonka, T. Przedzinski, and Z. Was. MC-TESTER v. 1.23: A Universal tool for comparisons of Monte Carlo predictions

- for particle decays in high energy physics. *Comput. Phys. Commun.*, 182:779–789, 2011.
- [6] N. Davidson, T. Przedzinski, and Z. Was. PHOTOS interface in C++: Technical and Physics Documentation. *Comput. Phys. Commun.*, 199:86–101, 2016.
- [7] Y. Jin et al. Observation of  $\tau^- \rightarrow \pi^- \nu_\tau e^+ e^-$  and search for  $\tau^- \rightarrow \pi^- \nu_\tau \mu^+ \mu^-$ . *Phys. Rev.*, D100(7):071101, 2019.
- [8] M. S. Alam et al. Tau decays into three charged leptons and two neutrinos. *Phys. Rev. Lett.*, 76:2637–2641, 1996.
- [9] A. Flores-Tlalpa, G. LÁspez Castro, and P. Roig. Five-body leptonic decays of muon and tau leptons. *JHEP*, 04:185, 2016.
- [10] Z. Was. Radiative corrections. In *1993 European School of High-Energy Physics, Zakopane, Poland, 12-25 Sep 1993: Proceedings*, pages 307–338, 1994.

## A Phase space parameters and presamplers

In this Appendix we describe the presampler parameters and how the phase space channels are prepared for each group of decays with distinct number of particles in the final state.

Firstly, we would like to point, that ordering of particles is important for proper functioning of the presampler. Therefore, the user should make sure that resonances in the matrix element are generated from four momenta of particles that can be constructed with resonant type phase space. Otherwise, the generation will suffer from extremely low efficiency or in severe cases generate incorrect distributions. Except for channels with neutrino-less decays, the last particle should be always set  $\nu_\tau$ . Neutrino-less decays can only be applied to channels with 2 or 3 particles in the final state.

Secondly, as mentioned in Section 2, it is important to note that although the phase space generators have multiple presampler channels, not all of them are always used. Depending on the probabilities in their parameterization, specific  $\tau$  decay channels can be activated.

In the following subsections, we will use the notation of  $M_{abc}^2$ , for example, to mean the invariant mass squared of system of 3 particles: a, b and

c, respectively, where a, b and c are numbers given while ordering them accordingly.

## A.1 Phase space for decays into 6 particles

Presampler for decays into 6 particles has up to 4 channels. Both, resonant and flat type phase space are present only for  $M_{12345}^2$  and  $M_{234}^2$ . The use of this type of parameterization is chosen randomly and independently of each other. Other invariant masses are generated using only the flat type presampler. Therefore, possible presampler channels are:

- flat  $M_{12345}^2 \rightarrow$  flat  $M_{1234}^2 \rightarrow$  flat  $M_{234}^2 \rightarrow$  flat  $M_{34}^2$ ,
- resonant  $M_{12345}^2 \rightarrow$  flat  $M_{1234}^2 \rightarrow$  flat  $M_{234}^2 \rightarrow$  flat  $M_{34}^2$ ,
- flat  $M_{12345}^2 \rightarrow$  flat  $M_{1234}^2 \rightarrow$  resonant  $M_{234}^2 \rightarrow$  flat  $M_{34}^2$ ,
- resonant  $M_{12345}^2 \rightarrow$  flat  $M_{1234}^2 \rightarrow$  resonant  $M_{234}^2 \rightarrow$  flat  $M_{34}^2$ .

The presampler parameters are:

- $P_A$  - probability of resonant type phase space in  $M_{12345}^2$ ,
- $P_B$  - probability of resonant type phase space in  $M_{234}^2$ ,
- MA - mass-like parameter for  $M_{12345}^2$ ,
- GA - width-like parameter for  $M_{12345}^2$ ,
- MB - mass-like parameter for  $M_{234}^2$ ,
- GB - width-like parameter for  $M_{234}^2$ .

## A.2 Phase space for decays into 5 particles

Presampler for  $\tau$  decays into 5 particles has up to 6 channels. Flat and resonant type phase space parameterization are present in the mass of three particles excluding  $\nu_\tau$ . The system is symmetrized for same type of particles in the first and second place giving 3 options here: flat parameterization in the invariant mass of three particles, resonant parameterization in the  $M_{234}^2$  and resonant parameterization in the  $M_{134}^2$ . If first and second particles

are different, the latter generation channel is discarded. Resonant type phase space is always used for the  $M_{1234}^2$ . Also, there are internally defined parameters for resonant type parameterization in the  $M_{34}^2$  (see section 4). Therefore, possible presampler channels are:

- resonant  $M_{1234}^2 \rightarrow$  flat  $M_{234}^2 \rightarrow$  flat  $M_{34}^2$ ,
- resonant  $M_{1234}^2 \rightarrow$  flat  $M_{234}^2 \rightarrow$  resonant  $M_{34}^2$ ,
- resonant  $M_{1234}^2 \rightarrow$  resonant  $M_{234}^2 \rightarrow$  flat  $M_{34}^2$ ,
- resonant  $M_{1234}^2 \rightarrow$  resonant  $M_{234}^2 \rightarrow$  resonant  $M_{34}^2$ ,
- resonant  $M_{1234}^2 \rightarrow$  resonant  $M_{134}^2 \rightarrow$  flat  $M_{34}^2$ ,
- resonant  $M_{1234}^2 \rightarrow$  resonant  $M_{134}^2 \rightarrow$  resonant  $M_{34}^2$ .

The presampler parameters available through user interface are:

- $P_A$  - probability of resonant type phase space in  $M_{234}^2$  and  $M_{134}^2$ ,
- $P_B$  - redundant parameter with same meaning as  $P_A$ ,
- MR - mass-like parameter for  $M_{1234}^2$ ,
- GR - width-like parameter for  $M_{1234}^2$ ,
- MA - mass-like parameter for  $M_{234}^2$  and  $M_{134}^2$ ,
- GA - width-like parameter for  $M_{234}^2$  and  $M_{134}^2$ ,

Probabilities  $P_A$  and  $P_B$  are summed up and the result is a probability of using resonant type phase space parameterization in the mass of three particles. Such structure was adopted due to the possible introduction of additional generation channel in the mass of three particles (mirroring other phase space generators), but the need to fully exploit this feature never arose. Then,  $P_A$  and  $P_B$  would have same function as in other phase space generators. Internally defined parameters are:  $M_{34} = 0.001$ ,  $\Gamma_{34} = 0.001$  and  $P_K$ , where  $P_K$  is probability of resonant type presampler set to 0.8 if the 3<sup>rd</sup> and the 4<sup>th</sup> particles are electron and positron, respectively. Otherwise it is set to 0.0, which means only flat type phase space in present in  $M_{34}^2$ .

### A.3 Phase space for decays into 4 particles

In case of channels with 4 particles in the final state, presampler has up to 3 channels. All the three channels use resonant type phase space parameterization for  $M_{123}^2$ . Channels A and B use parameterization for  $M_{13}^2$  or  $M_{23}^2$ , respectively, but with different parameters, while the third channel is uses flat type phase space in the invariant mass squared of two particles. Therefore, the possible presampler channels are:

- resonant  $M_{123}^2 \rightarrow$  resonant  $M_{13}^2$  (channel A),
- resonant  $M_{123}^2 \rightarrow$  resonant  $M_{23}^2$  (channel B),
- resonant  $M_{123}^2 \rightarrow$  flat  $M_{23}^2$ .

The presampler has following 8 parameters:

- $P_A$  - probability of channel A,
- $P_B$  - probability of channel B,
- MX - mass-like parameter for  $M_{123}^2$ ,
- GX - width-like parameter for  $M_{123}^2$ ,
- MA - mass-like parameter for channel A,
- GA - width-like parameter for channel A,
- MB - mass-like parameter for channel B,
- GB - width-like parameter for channel B.

The probability of channel with flat phase space in the mass of two particles equals  $1 - P_A - P_B$ . If  $P_A = P_B = 0.0$ , only the third channel is used.

### A.4 Phase space for decays into 3 particles

The presampler for decays into 3 particles has 3 channels, all of which differ only in the phase space parameterization used for the  $M_{12}^2$ . Therefore, possible presampler channels are:

- resonant  $M_{12}^2$  (channel A),

- resonant  $M_{12}^2$  (channel B),
- flat  $M_{12}^2$ .

The presampler has following parameters:

- $P_A$  - probability of channel A,
- $P_B$  - probability of channel B,
- $M_A$  - mass-like parameter for channel A,
- $G_A$  - width-like parameter for channel A,
- $M_B$  - mass-like parameter for channel B,
- $G_B$  - width-like parameter for channel B.

Probability of flat phase space (third channel) in the  $M_{12}^2$  equals  $1 - P_A - P_B$ .

### A.5 Phase space for decays into N and 2 particles

Presamplers for decays into 2 and N particles do not have any parameters. Decay into 2 particles does not need parameters for obvious reason. Presampler for N particles can be used for up to 9 particles in final state but always uses flat phase space for invariant mass squared of every system with descending number of particles e.g. for  $N=9$ :  $M_{12345678}^2, M_{2345678}^2, \dots, M_{678}^2, M_{78}^2$ . Use of matrix element is restricted.

## B Technical tests for phase space and pair emission in $\tau^- \rightarrow \bar{\nu}_\mu \mu^- \nu_\tau$

In this appendix we collect the formulae which numerical algorithm of TAUOLA [1] relies on. They also provide platform to perform tests. We focus on a pair of channels  $\tau^- \rightarrow \bar{\nu}_\mu \mu^- \nu_\tau$  and  $\tau^- \rightarrow \bar{\nu}_\mu \mu^- e^- e^+ \nu_\tau$ , but obtained formulae are of use for  $\tau^- \rightarrow \bar{\nu}_e e^- \nu_\tau$  and  $\tau^- \rightarrow \bar{\nu}_e e^- e^- e^+ \nu_\tau$  channels as well. The second channel in each pair differs from the first by the presence of a  $e^- e^+$  pair and can be understood as a contribution to bremsstrahlung correction. The dominant contribution is due to  $e^- e^+$  pair of small virtuality (originating from the decay of nearly real photon). In calculations we use in general

notation of [10]. We shorten:  $\bar{\nu}$  mean  $\bar{\nu}_\ell$ , where  $\ell$ , either electron or muon, and  $\nu$  means  $\nu_\tau$ .

### 3 body decay

An integral of matrix element squared  $|M|^2 \equiv |M(p_\tau, p_\nu, p_{\bar{\nu}}, p_\mu)|^2$  over 3-body phase space  $dLips_3(p_\tau, p_\nu, p_{\bar{\nu}}, p_\mu)$  reads:

$$\begin{aligned} \int |M|^2 dLips_3(p_\tau, p_\nu, p_{\bar{\nu}}, p_\mu) &= \int |M|^2 \frac{d^3 p_\nu}{(2\pi)^3 2p_\nu^0} \frac{d^3 p_{\bar{\nu}}}{(2\pi)^3 2p_{\bar{\nu}}^0} \frac{d^3 p_\mu}{(2\pi)^3 2p_\mu^0} (2\pi)^4 \delta^4(p_\tau - p_\nu - p_{\bar{\nu}} - p_\mu) = \\ &= \frac{1}{2^{11} \pi^5} \int_{m_\mu^2}^{(m_\tau - m_\mu)^2} dM_{\bar{\nu}\mu}^2 \int_{-1}^1 d\cos\theta_\nu \int_0^{2\pi} d\varphi_\nu \left(1 - \frac{M_{\bar{\nu}\mu}^2}{m_\tau^2}\right) \int_{-1}^1 d\cos\theta_{\bar{\nu}} \int_0^{2\pi} d\varphi_{\bar{\nu}} \left(1 - \frac{m_\mu^2}{M_{\bar{\nu}\mu}^2}\right) |M|^2, \end{aligned} \quad (9)$$

where  $p_\tau, p_\nu, p_{\bar{\nu}}, p_\mu$  are four-momenta of  $\tau^-$ ,  $\nu$ ,  $\bar{\nu}_\mu$ ,  $\mu^-$  correspondingly;  $d\cos\theta_\nu d\varphi_\nu$  is the solid angle element of  $p_\nu$  in the rest frame of  $\tau^-$ ,  $d\cos\theta_{\bar{\nu}} d\varphi_{\bar{\nu}}$  is the solid angle element of  $p_{\bar{\nu}}$  in the rest frame of  $(p_{\bar{\nu}} + p_\mu)$ ;  $M_{\bar{\nu}\mu}^2 = (p_{\bar{\nu}} + p_\mu)^2$ ;  $m_\mu$  is mass of  $\mu^-$  and  $m_\tau$  is mass of  $\tau^-$ .

### 5 body decay

We proceed with writing a cross section for the 5-body decay  $\tau^- \rightarrow \bar{\nu}_\mu \mu^- e^- e^+ \nu_\tau$  assuming the matrix element  $|M|^2 \equiv |M(p_\tau, p_{e-}, p_{e+}, p_\nu, p_{\bar{\nu}}, p_\mu)|^2$  can be factorized. We focus on soft pair emissions:

$$|M|^2 = |M(p_\tau, p_\nu, p_{\bar{\nu}}, p_\mu)|^2 \times |M_F(p_{e-}, p_{e+})|^2. \quad (10)$$

Therefore:

$$\begin{aligned} \int |M|^2 dLips_5(p_\tau, p_{e-}, p_{e+}, p_\nu, p_{\bar{\nu}}, p_\mu) &= \\ &= \int |M_F|^2 \frac{d^3 p_{e-}}{(2\pi)^3 2p_{e-}^0} \frac{d^3 p_{e+}}{(2\pi)^3 2p_{e+}^0} d^4 R \delta^4(R - p_\tau + p_{e-} + p_{e+}) \times \\ &\times \int |M(p_\tau, p_\nu, p_{\bar{\nu}}, p_\mu)|^2 \frac{d^3 p_\nu}{(2\pi)^3 2p_\nu^0} \frac{d^3 p_{\bar{\nu}}}{(2\pi)^3 2p_{\bar{\nu}}^0} \frac{d^3 p_\mu}{(2\pi)^3 2p_\mu^0} (2\pi)^4 \delta^4(R - p_\nu - p_{\bar{\nu}} - p_\mu), \end{aligned} \quad (11)$$

where  $p_\tau, p_{e-}, p_{e+}, p_\nu, p_{\bar{\nu}}, p_\mu$  are four-momenta of  $\tau^-$ ,  $e^-$ ,  $e^+$ ,  $\nu$ ,  $\bar{\nu}_\mu$ ,  $\mu^-$  correspondingly. At first and for a test, we put  $|M_F|^2 \equiv 1$ . Since the factorized part of matrix element squared  $|M_F|^2$  does not depend on  $p_{e-}, p_{e+}$  anymore, for a soft pair emission we can drop  $e^+$  and  $e^-$  from the conditions of momentum-energy conservation. Thus the technical integral element  $d^4 R \delta^4(R - p_\tau + p_{e-} + p_{e+})$  reduces to  $R = p_\tau$  and

$$\begin{aligned}
& \int |M|^2 dLips_5(p_\tau, p_{e-}, p_{e+}, p_\nu, p_{\bar{\nu}}, p_\mu) \approx \\
& = \int \frac{d^3 p_{e-}}{(2\pi)^3 2p_{e-}^0} \frac{d^3 p_{e+}}{(2\pi)^3 2p_{e+}^0} \int |M|^2 dLips_3(p_\tau, p_\nu, p_{\bar{\nu}}, p_\mu) = \\
& = \frac{1}{2^8 \pi^6} \int \left[ d\cos\theta_{e-} d\varphi_{e-} \frac{|\bar{p}_{e-}|^2 d|\bar{p}_{e-}|}{\sqrt{|\bar{p}_{e-}|^2 + m_e^2}} \right]_{\bar{p}_\tau=0} \left[ d\cos\theta_{e+} d\varphi_{e+} \frac{|\bar{p}_{e+}|^2 d|\bar{p}_{e+}|}{\sqrt{|\bar{p}_{e+}|^2 + m_e^2}} \right]_{\bar{p}_\tau=0} \times \\
& \times \int |M(p_\tau, p_\nu, p_{\bar{\nu}}, p_\mu)|^2 dLips_3(p_\tau, p_\nu, p_{\bar{\nu}}, p_\mu), \tag{12}
\end{aligned}$$

where  $\bar{p}_{e-}$ ,  $\bar{p}_{e+}$  are three-momenta of  $e^-$ ,  $e^+$  correspondingly; subscript  $\bar{p}_\tau = 0$  or  $\bar{p}_\nu + \bar{p}_\mu = 0$  means that the variables into square brackets are in  $\tau^-$  rest frame;  $d\cos\theta_{e-} d\varphi_{e-}$  is the solid angle element of  $p_{e-}$ ,  $d\cos\theta_{e+} d\varphi_{e+}$  is the solid angle element of  $p_{e+}$ .

Our formula is valid for soft  $e^+e^-$  only, that is why we can work only with a part of the phase space. We introduce a cutoff parameter  $\Delta_1$ :  $p_{e+}^0 < \Delta_1$ ,  $p_{e-}^0 < \Delta_1$ . Such conditions match the limitation introduced for the TAUOLA generation. We obtain:

$$\int |M|^2 dLips_5(p_\tau, p_{e-}, p_{e+}, p_\nu, p_{\bar{\nu}}, p_\mu) \approx \frac{\Delta_1^4}{2^6 \pi^4} \int |M|^2 dLips_3(p_\tau, p_\nu, p_{\bar{\nu}}, p_\mu) \tag{13}$$

and soft pair emission factor of the test reads:

$$B_f(\Delta_1) \approx \frac{\Delta_1^4}{2^6 \pi^4}. \tag{14}$$

Alternatively, the second test with  $|M_F|^2 \equiv 1$  is to write cross section for the 5-body decay in terms of invariant mass variables:

$$\int |M|^2 dLips_5(p_\tau) = \frac{1}{2^{11} \pi^5} \int dM_{\bar{\nu}\mu ee}^2 \int d\Omega_\nu \left(1 - \frac{M_{\bar{\nu}\mu ee}^2}{m_\tau^2}\right) \int d\Omega_{\bar{\nu}} \left(1 - \frac{M_{\mu ee}^2}{M_{\bar{\nu}\mu ee}^2}\right) |M(p_\tau, p_\nu, p_{\bar{\nu}}, p_\mu)|^2 \times \tag{15}$$

$$\times \frac{1}{2^{12} \pi^6} \int d\Omega_\mu \int d\Omega_e \int dM_{ee}^2 |M_F|^2 \sqrt{1 - \frac{4m_e^2}{M_{ee}^2}} \int dM_{\mu ee}^2 \frac{\sqrt{(M_{\mu ee}^2 - M_{ee}^2 - m_\mu^2)^2 - 4M_{ee}^2 m_\mu^2}}{M_{\mu ee}^2}, \tag{16}$$

where  $M_{\bar{\nu}\mu ee}^2 = (p_{\bar{\nu}} + p_\mu + p_{e-} + p_{e+})^2$ ,  $M_{\mu ee}^2 = (p_\mu + p_{e-} + p_{e+})^2$ ,  $M_{ee}^2 = (p_{e-} + p_{e+})^2$ ;  $d\Omega_\nu$  is the solid angle element of  $p_\nu$  in the rest frame of  $\tau^-$ ,  $d\Omega_{\bar{\nu}}$

is the solid angle element of  $p_{\bar{\nu}}$  in the rest frame of  $(p_{e-} + p_{e+} + p_{\bar{\nu}} + p_{\mu})$ ,  $d\Omega_{\mu}$  is the solid angle element of  $p_{\mu}$  in the rest frame of  $(p_{e-} + p_{e+} + p_{\mu})$ ,  $d\Omega_e$  is the solid angle element of  $p_{e-}$  in the rest frame of  $(p_{e-} + p_{e+})$ . Considering pair emission is soft, we can approximate  $M_{\bar{\nu}\mu ee}^2 \approx M_{\bar{\nu}\mu}^2$ ,  $M_{\mu ee}^2 = m_{\mu}^2$ , thus first part of cross section (15) coincide with cross section (9) for 3-body decay  $\tau^- \rightarrow \bar{\nu}_{\mu}\mu^-\nu_{\tau}$ . Soft pair emission factor reads:

$$B_f(\Delta_2) = \frac{1}{2^8 \pi^4} \int_{\frac{4m_e^2}{M_{ee}^2}}^{\Delta_2^2} dM_{ee}^2 \sqrt{1 - \frac{4m_e^2}{M_{ee}^2}} \int_{\frac{(m_{\mu} + \Delta_2)^2}{(m_{\mu} + M_{ee})^2}}^{\frac{(m_{\mu} + \Delta_2)^2}{(m_{\mu} + M_{ee})^2}} dM_{\mu ee}^2 \frac{\sqrt{\left(M_{\mu ee}^2 - M_{ee}^2 - m_{\mu}^2\right)^2 - 4M_{ee}^2 m_{\mu}^2}}{M_{\mu ee}^2}. \quad (17)$$

Here cutoff  $\Delta_2$  limits invariant mass of the  $e^+e^-$  pair, therefore cutoff could be invoked in TAUOLA easily. Double integral of soft pair emission factor Eq. (17) doesn't have a simple analytical solution. On the other hand, numerical solution works perfectly for testing purposes.

The  $B_f$  of Eq. (17) as function of  $\Delta_2$  can be easily translated into  $\Delta_2$  dependent partial widths simply multiplying partial width of  $\tau^- \rightarrow \bar{\nu}_{\mu}\mu^-\nu_{\tau}$  decay by  $B_f(\Delta_2)$ . Results obtained that way and those from Monte Carlo simulation are collected in Table 7. They provide also a test of approach used in Eq. (10) - tests with simplified matrix element.

$\Delta_2$ [GeV]	Partial width [GeV]	
	$B_f(\Delta_2) \times \Gamma(\tau \rightarrow \bar{\nu}\mu\nu)$	Monte Carlo
0.00125	$0.42866 \cdot 10^{-30}$	$0.42729 \cdot 10^{-30}$
0.0025	$0.16289 \cdot 10^{-27}$	$0.15965 \cdot 10^{-27}$
0.005	$0.48627 \cdot 10^{-26}$	$0.46480 \cdot 10^{-26}$
0.01	$0.92486 \cdot 10^{-23}$	$0.84837 \cdot 10^{-23}$
0.02	$0.15208 \cdot 10^{-22}$	$0.12664 \cdot 10^{-22}$

Table 7: Partial width obtained for different cutoff  $\Delta_2$  from Monte Carlo run and numerically from  $B_f$  of Eq.(17). Note, that with increasing cutoff  $\Delta_2$ , pairs are allowed to be somewhat harder, therefore assumption  $\Gamma(\tau \rightarrow \bar{\nu}\mu ee\nu) \approx B_f * \Gamma(\tau \rightarrow \bar{\nu}\mu\nu)$ . Uncertainty of MC results is at the level of 1%.

Similar tests with  $|M_F|^2$  closer to a physical model can be also performed. Results for all such comparisons would be redundant, therefore we present only next step, where we choose factorized part of matrix element squared to be:  $|M_F|^2 = \frac{(4\pi\alpha)^2}{(p_{e+} + p_{e-})^2}$ . Such a choice should represent numerical effects of a

singular behavior during simulation of soft pair emission. Soft pair emission factor in this case reads:

$$\begin{aligned}
B_f &= \int |M_F|^2 \frac{d^3 p_{e-}}{(2\pi)^3 2p_{e-}^0} \frac{d^3 p_{e+}}{(2\pi)^3 2p_{e+}^0} d^4 R \delta^4(R - p_\tau + p_{e-} + p_{e+}) = \\
&= \frac{1}{(2\pi)^6} \int \frac{(4\pi\alpha)^2}{q^2} \frac{d^3 p_{e-}}{2p_{e-}^0} \frac{d^3 p_{e+}}{2p_{e+}^0} d^4 q dM_{ee}^2 \delta(q^2 - M_{ee}^2) \Theta(q^0) \times \\
&\quad \times \delta^4(q - p_{e+} - p_{e-}) d^4 R dM_{\mu\nu\bar{\nu}}^2 \delta(R^2 - M_{\mu\nu\bar{\nu}}^2) \Theta(R^0) \delta^4(R - p_\tau + q), \quad (18)
\end{aligned}$$

where we've introduced  $q = p_{e-} + p_{e+}$ ;  $R = p_\nu + p_{\bar{\nu}} + p_\mu$ , which represents 4-momentum of rest of the particles system after pair emission takes place, and invariant mass squares  $M_{ee}^2 = (p_{e+} + p_{e-})^2$  and  $M_{\mu\nu\bar{\nu}}^2 = (p_\nu + p_{\bar{\nu}} + p_\mu)^2$ . With help of formulae

$$\begin{aligned}
\int \frac{d^3 p_{e-}}{2p_{e-}^0} \frac{d^3 p_{e+}}{2p_{e+}^0} d^4 q \delta^4(q - p_{e+} - p_{e-}) &= \int d^4 q d\cos\theta_1 d\varphi_1 \frac{1}{8} \sqrt{1 - \frac{4m_e^2}{q^2}}, \\
\int d^4 q dM_{ee}^2 \delta(q^2 - M_{ee}^2) \Theta(q^0) &= \int \frac{d^3 q}{2q^0}, \\
\int d^4 R dM_{\mu\nu\bar{\nu}}^2 \delta(R^2 - M_{\mu\nu\bar{\nu}}^2) \Theta(R^0) &= \int \frac{d^3 R}{2R^0} \quad (19)
\end{aligned}$$

$B_f$  reads:

$$B_f = \frac{\alpha^2}{2^3 \pi^3} \int \frac{dM_{ee}^2}{M_{ee}^4} \sqrt{1 - \frac{4m_e^2}{M_{ee}^2}} dM_{\mu\nu\bar{\nu}}^2 d\cos\theta_2 d\varphi_2 \frac{\lambda^{1/2}(m_\tau^2, M_{ee}^2, M_{\mu\nu\bar{\nu}}^2)}{8m_\tau^2}, \quad (20)$$

$$\text{where } \lambda^{1/2}(m_\tau^2, M_{ee}^2, M_{\mu\nu\bar{\nu}}^2) = \sqrt{(m_\tau^2 + M_{ee}^2 - M_{\mu\nu\bar{\nu}}^2)^2 - 4m_\tau^2 M_{\mu\nu\bar{\nu}}^2}.$$

Integration over angular variables performs trivially. An easy way to proceed with integration is to integrate over energy  $E_{ee} = \frac{m_\tau^2 + M_{ee}^2 - M_{\mu\nu\bar{\nu}}^2}{2m_\tau}$  of the pair in the rest frame of  $\tau^-$ . For the condition  $dM_{ee}^2 = 0$ , differential of the energy of the pair reads  $dE_{ee} = -\frac{dM_{\mu\nu\bar{\nu}}^2}{2m_\tau}$  leading to  $\lambda^{1/2}(m_\tau^2, M_{ee}^2, M_{\mu\nu\bar{\nu}}^2) = 2m_\tau \sqrt{E_{ee}^2 - M_{ee}^2}$ .

Soft pair emission factor reads:

$$\begin{aligned}
B_f(\Delta_3) &= \frac{\alpha^2}{2^2\pi^2} \int_{4m_e^2}^{\Delta_3^2} \frac{dM_{ee}^2}{M_{ee}^2} \sqrt{1 - \frac{4m_e^2}{M_{ee}^2}} \int_{M_{ee}}^{\Delta_3} dE_{ee} \sqrt{E_{ee}^2 - M_{ee}^2} = \\
&= \frac{\alpha^2}{2^3\pi^2} \int_{4m_e^2}^{\Delta_3^2} \frac{dM_{ee}^2}{M_{ee}^2} \sqrt{1 - \frac{4m_e^2}{M_{ee}^2}} \left( \Delta_3 \sqrt{\Delta_3^2 - M_{ee}^2} + M_{ee}^2 \ln \frac{M_{ee}}{\Delta_3 + \sqrt{\Delta_3^2 - M_{ee}^2}} \right), \quad (21)
\end{aligned}$$

where  $\Delta_3$ , maximal energy of the pair in the  $\tau^-$  rest frame determines the  $\Delta_3^2$  the maximal  $M_{ee}^2$ . Analytical expression for  $B_f(\Delta_3)$  for this choice of  $|M_F|^2$  is long and is not instructive. Partial widths obtained using this new  $B_f(\Delta_3)$  and those from Monte Carlo simulation are collected in Table 8.

$\Delta_3$ [GeV]	Partial width [GeV]	
	$B_f(\Delta_3) \times \Gamma(\tau \rightarrow \bar{\nu}\mu\nu)$	Monte Carlo
0.0025	$0.59970 \cdot 10^{-24}$	$0.59826 \cdot 10^{-24}$
0.005	$0.82769 \cdot 10^{-23}$	$0.81803 \cdot 10^{-23}$
0.01	$0.64485 \cdot 10^{-22}$	$0.64446 \cdot 10^{-22}$
0.02	$0.39679 \cdot 10^{-21}$	$0.38269 \cdot 10^{-21}$

Table 8: Partial width obtained for different cutoff  $\Delta_3$  from Monte Carlo run and numerically from  $B_f$  of Eq.(21). Note, that with increasing cutoff  $\Delta_3$ , pairs are allowed to be somewhat harder therefore assumption  $\Gamma(\tau \rightarrow \bar{\nu}\mu\mu\tau) \approx B_f * \Gamma(\tau \rightarrow \bar{\nu}\mu\nu)$  works worse. Uncertainty of MC results is at the level of 1%. Those results, together with the ones collected in Table 7, provide us with confirmation that approach of Eq. (10) is justified as well as provide technical test for the phase space generation in TAUOLA.